PERGAMON

International Journal of Multiphase Flow 27 (2001) 189–196

International Journal of Multiphase Flow

www.elsevier.com/locate/ijmulflow

Brief communication

On the influence of mass transfer on coalescence of bubbles

A.M. Leshansky

Department of Chemical Engineering, Technion - I.I.T., Haifa 32000, Israel

Received 4 August 1997; received in revised form 28 December 1999

1. Introduction

The contact area between disperse and continuous fluids is one of the key parameters controlling mass transfer in numerous technological operations. Since the disperse phase size distribution is mainly a result of the disperse phase fluid particle coalescence the modeling of that phenomenon becomes particularly important. As reported, the critical gas flow in the bubble columns, at which flow transition from bubble flow to recirculating turbulent flow occurs, can be correlated with coalescence time (Ueyama et al., 1993). It is known for some years that the direction of solute mass transfer can be responsible for the drastic change in the rate of coalescence between liquid drops immersed into the continuous phase fluid (see Groothuiz and Zuiderweg, 1960; Jeffreys and Lawson, 1965; Gourdon and Casamatta, 1991). The main conclusion from these experimental works can be formulated as follows: a progressive decrease in drops stability was noticed in the case of increased diffusion rate *from* the drops, whereas a progressive increase in stability was shown to occur where diffusion takes place *into* the drops for increasing rates of solute mass transfer. Velev et al. (1993) observed a spontaneous cyclic phenomenon of dimple formation in aqueous emulsion films accompanied by interphase mass transfer. In these experiments a dilute nonionic surfactant was transferred from the aqueous emulsion film toward the surrounding oil phases. The process of dimpling goes for hours until the surfactant distribution is equilibrated, then the film quickly thins and ruptures. Recently, Danov et al. (1997) proposed a hydrodynamic description for the above phenomenon of spontaneous dimpling based on a lubrication theory, which can predict satisfactorily the final steady shape of a dimple, but does not reflect the cyclic nature of dimpling. It was shown that the Marangoni effect is responsible for the dimple growth and,

E-mail address: lisha@techunix.technion.ac.il (A.M. Leshansky).

0301-9322/01/$ - see front matter
PII: S0301-9322(00)00013-6

thus, for the high stability of non-equilibrium emulsion films that are accompanied by outward surfactant transfer.

The onset of the Marangoni instability due to solute transport has been studied extensively for the case of single interface liquid–liquid or liquid–gas systems (Sternling and Scriven, 1959; England and Berg, 1971; Sorensen et al., 1977; Hennenberg et al., 1977; and recently Slavtchev et al., 1998), while it has not been studied in detail for the case of multiple interface systems.

The aim of this paper is to develop a simplified theoretical description which will be able to explain the difference in relative stability of inter-particle liquid film due to the *direction* of mass transfer. A simple hydrodynamic model is derived and studied by means of a linear stability analysis of a narrow *flat* layer of liquid between two semi-infinite gas phases. A surface active solute is assumed to cross the interface either from the gas phase into the liquid layer or vice versa.

This model can be addressed to coalescence of two bubbles under a number of simplifying assumptions. First, the *hydrodynamic interaction* between bubbles during their approach is neglected. In fact, when the separation distance, d, between the bubbles tends to zero, the viscous force acting on them grows fast and the velocity of their approach tends to zero as $d^{1/2}$ in the limit of high surface tension (Lavrenteva et al., 1999). Second, the narrow liquid film which develops between the deformed bubbles is regarded as a plain sheet.

Recent experiments on bubble coalescence, using laser measuring technique by Ueyama et al. (1993) confirm that the approach velocity and bubble size (i.e., curvature effects) have only a minor effect on the coalescence time, while the initial solutal distribution between bubbles and surrounding liquid phase has a strong influence on it.

2. Problem formulation

Consider a quiescent two-dimensional layer of incompressible liquid which is infinite in horizontal direction and bounded vertically by the two *free* liquid–gas surfaces. The width of the layer is h_0, the surface tension is σ_0, the density and the kinematic viscosity of the liquid are ρ and ν, respectively. Suppose that there are no body forces. Two qualitatively different cases are under study: (i) solute is transferred across the interface toward the gas phases, called 1, (into the bubbles); (ii) solute is transferred across the interfaces toward the liquid layer, called 2. The transferring substance is either a *weakly surface active* solute (solutal molecules consist of short hydrophobic tail and weakly polar hydrophilic head, e.g., acetic acid, ethanol, acetone etc.) or a very dilute *strong surfactant* (surfactant molecules consist of long hydrophobic tail with polar head). In both cases the solute adsorption at the interface is small and the hindering effect on the mobility of the interface is negligible, while it still influencing the local surface tension. In the latter case, the scale of excess-solute interfacial concentration, Γ_0^*, must satisfy $\Gamma_0^* \ll \Gamma_m^*$, where Γ_m^* is the critical *micelle* concentration. We assume that the solute mass transfer is controlled by the bulk diffusion in liquid phase and by adsorption–desorption rate in gas phase; the solute diffusion in the gas is much faster than that in the liquid. In such cases: $\frac{d^2/D_2}{d/k_2}$, $\frac{d^2/D_2}{1/k_{-2}} \gg 1$, $\frac{d^2/D_1}{d/k_1}$, $\frac{d^2/D_1}{1/k_{-1}} \ll 1$ and $D_2/D_1 \ll 1$ where D_i are the solute diffusivities in ith phase, k_i and k_{-i} are the kinetic rates of adsorption and desorption of solute in ith phase, respectively, and d is the characteristic length of the problem. In phase 2

the mass fluxes are controlled by the concentration gradients, while the adsorption–desorption processes at the interfaces are in local equilibrium. In phase 1 the mass fluxes are determined by the adsorption–desorption rates on the gas side of the interfaces, while the concentration gradients are negligible due to the fast bulk diffusion (e.g., if acetone, triethylamine or diethylether desorbs from water into air bubbles, $D_{\rm air}/D_{\rm water}\sim 10^{-4}$). Thus, the excess-solute interfacial concentration, Γ^*, is proportional to the bulk concentration along the liquid side of the interface, $\Gamma^*\sim\delta_2 C_2$ and $\delta_2\sim k_2/k_{-2}$.

All physical properties of the ambient fluid are assumed to be constant, except for the surface tension, which depends linearly on the excess-solute interfacial concentration: $\sigma=\sigma_0+(\partial\sigma/\partial\Gamma^*)_0(\Gamma^*-\Gamma_0)$, where Γ_0 and σ_0 are reference positive values and $(\partial\sigma/\partial\Gamma^*)_0<0$ for the surface-tension-lowering solute. While the excess-solute interfacial concentration is in local equilibrium with the solute in adjacent liquid sublayers, $\sigma\sim\sigma_0+(\partial\sigma/\partial\Gamma^*)(\delta_2C_2-\Gamma_0)=\sigma_0+\sigma'(C_2-C^*)$.

At the liquid–gas interfaces we assume that the Robin type boundary condition holds in both cases. In case (i) of solute desorption from the continuous liquid phase into bubbles,

$$z=1,0:\quad \pm D_2\frac{\partial C_2}{\partial z}=K_{\rm G}(C_1/m-C_2), \tag{1}$$

and in case (ii) of solute adsorption by the continuous liquid phase from the bubbles,

$$z=1,0:\quad \pm D_2\frac{\partial C_2}{\partial z}=K_{\rm G}(C_1-C_2m), \tag{2}$$

where $K_{\rm G}$ is the gas-phase mass transfer coefficient (Rabinovich and Struchenko, 1993), which can be attributed to the first-order adsorption–desorption kinetics as $K_{\rm G}=k_{-1}\delta_2$ in case (i) and as $K_{\rm G}=k_1$ in case (ii); m is Henry's constant and C_1 denotes the *constant* concentration of solute in the gas phase.

The gas viscosity is ignored and only the flow inside the liquid layer is considered. We scale length, time, velocity and pressure in units of h_0, h_0^2/ν, ν/h_0 and $\rho\nu^2/h_0^2$, respectively. In case (i) we choose the dimensionless concentration of solute in phase 2 as $\theta=(C_2-C_1/m)/(C_{20}-C_1/m)$, where C_{20} is the initial concentration of the surface active solute in the liquid layer. In case (ii) we define $\theta=(C_1/m-C_2)/(C_1/m-C_{20})$.

In a quiescent state the mass transfer of solute is controlled by diffusion and in both cases the governing equations and the boundary conditions for the dimensionless concentration read,

$$\frac{\partial\theta_0}{\partial t}=\frac{1}{Sc}\nabla^2\theta_0 \tag{3}$$

$$z=1,0:\quad \frac{\partial\theta_0}{\partial z}\pm\chi Sh\,\theta_0=0 \tag{4}$$

$$0<z<1:\quad \theta_0(z,0)=1 \tag{5}$$

where z and t are, respectively, a dimensionless transverse coordinate and time. The dimensionless groups of the problem are the Schmidt number $Sc=\nu/D_2$, the Sherwood

number $Sh = K_G h_0/D_2$, $\chi = 1$ in case (i) and $\chi = m$ in case (ii). The solution of this problem is given by Carslaw and Jaeger (1960)

$$\theta_0 = 2\sum_{n=1}^{\infty} \exp\left[-\alpha_n^2 t/Sc\right] \frac{\alpha_n \cos(\alpha_n z) + \chi Sh \sin(\alpha_n z)}{\alpha_n^2 + (\chi Sh)^2 + 2\chi Sh} \int_0^1 \left(\alpha_n \cos(\alpha_n s) + \chi Sh \sin(\alpha_n s)\right) \mathrm{d}s \tag{6}$$

where the coefficients α_n are the union of the positive roots of the following equations

$$\alpha \tan \alpha/2 - \chi Sh = 0, \qquad \alpha \cot \alpha/2 + \chi Sh = 0 \tag{7}$$

The dimensionless linearized equations and the boundary conditions (normal and tangential stress balance, kinematic condition and the solute transfer) governing the development of an arbitrary infinitesimal small perturbation for case (i) take the form

$$\partial_t \partial_z^2 v + \partial_t \partial_x^2 v = \partial_z^4 v + 2\partial_z^2 \partial_x^2 v + \partial_x^4 v, \tag{8}$$

$$\partial_t \theta + v\, \partial_z \theta_0 = \frac{1}{Sc}\left(\partial_x^2 \theta + \partial_z^2 \theta\right), \tag{9}$$

$$z = 1, 0: \quad \partial_t \partial_z v - \partial_z^3 v - 3\partial_z \partial_x^2 v = \mp (W - Ma\, \theta_0)\, \partial_x^4 h_\pm, \tag{10}$$

$$\partial_x^2 v - \partial_z^2 v = \mp\, Ma\left(\partial_x^2 \theta + \partial_z \theta_0\, \partial_x^2 h_\pm\right), \tag{11}$$

$$v = \partial_t h_\pm, \tag{12}$$

$$\partial_z \theta \pm \chi Sh\, \theta = \mp(\chi Sh\, \partial_z \theta_0 \pm \partial_{zz} \theta_0) h_\pm, \tag{13}$$

where x, v, θ, h_+, h_- are respectively dimensionless spatial longitudinal coordinate, transverse velocity, concentration deviation from the conductive state (6) and the distortion of the upper and lower free surfaces. Ma denotes the Marangoni number: $Ma = -\sigma' h_0 \Delta C/\rho\nu^2$, where $\Delta C = C_{20} - C_1/m$ and W stands for the crispation number: $W = h_0(\sigma_0 + \sigma'(C_1/m - C^*))/\rho\nu^2$. The formulation of problem (ii) is easily obtained from Eqs. (8)–(13) by the substitution $Ma \rightarrow -Ma$ (in case (ii) $Ma = -\sigma' h_0 \Delta C/\rho\nu^2$, where $\Delta C = C_1/m - C_{20}$).

Eq. (8) is obtained by, first, taking the rotor of the linearized NS equation to eliminate the pressure and, second, using the continuity equation to eliminate the x-component of the velocity; Eq. (9) represents the convection-diffusion equation for the conservation of the solute concentration disturbance. Eq. (10) is obtained after eliminating the pressure from the normal stress balance by first, taking an x-derivative and making use of the x-component of the momentum equation, followed by a second differentiation with respect to x and use of the continuity equation to eliminate the x-component of the velocity. The balance (11) is obtained after differentiating the tangential stress balance with respect to x and using of the continuity equation to eliminate the x-component of the velocity.

Applying normal mode analysis and expanding all variables in Eqs. (10)–(13) near the *unperturbed* boundaries $z = 0, 1$ yield the eigenvalue problem

$$\lambda(V'' - k^2 V) = V'''' - 2k^2 V'' + k^4 V, \tag{14}$$

$$\lambda\Theta + V\partial_z\theta_0 = \frac{1}{Sc}(\Theta'' - k^2\Theta), \tag{15}$$

$$z = 1, 0: \quad \lambda V' - V''' + 3k^2 V' = \mp H_{\pm} k^4 (W - Ma\,\theta_0), \tag{16}$$

$$V'' + k^2 V = \mp Ma\,k^2\left(\Theta + H_{\pm}\partial_z\theta_0\right), \tag{17}$$

$$V = \lambda H_{\pm}, \tag{18}$$

$$\Theta' \pm \chi Sh\,\Theta = \mp\left(\chi Sh\,\partial_z\theta_0 \pm \partial_z^2\theta_0\right) H_{\pm} \tag{19}$$

where $V(z), \Theta(z), H_+$ and H_- denote the amplitudes of velocity, concentration, upper and lower boundary perturbations, respectively; λ is the perturbation growth rate and k is the perturbation wavenumber. Prime stands for the differentiation with respect to z. Deriving Eqs. (14)–(19) we have assumed that the reference concentration profile (6) changes on a slow time scale, in other words the time changes in θ_0 are negligible during the initial stage of perturbation evolution. Thus we treat the time of disturbance onset, t_0, as parameter and "freeze" θ_0 at t_0. while the disturbance develops on a fast time scale t. The asymptotic estimates of α_1 are easily obtained from Eq. (7). When $\chi Sh \ll 1$ it follows that $\alpha_1 \sim \sqrt{2\chi Sh}$ and when $\chi Sh \gg 1$, $\alpha_1 \sim \pi\chi Sh/(\chi Sh + 2)$. Since the present stability analysis is valid for times: $t \ll Sc/\alpha_1^2$, Sc number is usually large (10^3–10^4) and α_1 is bounded by π from above for any value of χSh, it follows that "freezing" the reference concentration profile is justified for rather wide time range. Such an approach is often applied when the stability of an unsteady reference state is considered (Dijkstra and van de Vooren, 1985) and leads to an eigenvalue problem with constant coefficients.

3. Results and discussion

We first investigate the onset of a stationary instability corresponding to $\lambda = 0$ in Eqs. (14)–(19). Solving the Eqs. (14) and (15) in terms of hyperbolic functions and applying the solvability condition yield the marginal (neutral) stability curves $Ma_n = Ma_n(k)$. All calculations are done by the symbolic program *Mathematica*. Although, we obtained the expressions for those curves in closed from, they are rather cumbersome and are not given here. Typical marginal stability curves are plotted in Figs. 1 and 2, for three different reference times $t_0 = 2.5$, 10, and 50, and some values of parameters W, Sc and χSh. Fig. 1 corresponds to the case (i) when solute is transferred across the interfaces toward the gas phases, Fig. 2 relates to case (ii), when solute is transferred toward the liquid phase. For the former case (i), the instability occurs through so called *stretching* (ST) mode ($H_+ = H_-$). In Fig. 1 there is a range of Ma numbers for which the system is stable to long-wave perturbations and the curve has a minimum at some finite $k = k_{cr}(t_0)$. The asymptotic evaluation of Ma_n in the vicinity of

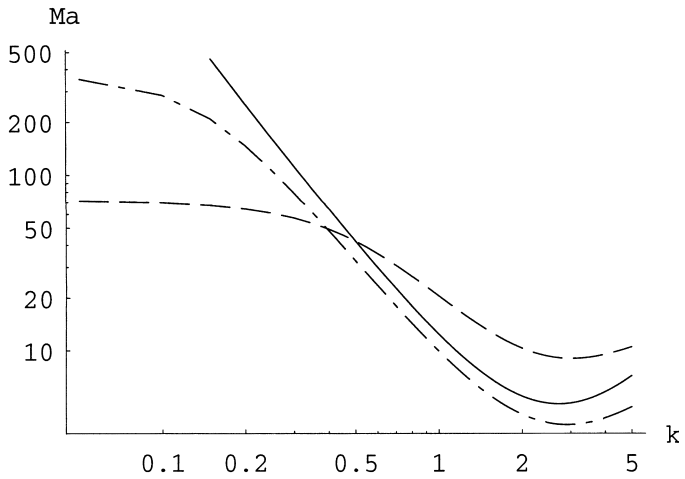

Fig. 1. Neutral stability curves for case (i) — solute desorbs into the gas phase, $W = 500$, $Sc = 100$ and $Sh = 5$. The dashed curve relates to the reference time $t_0 = 2.5$, the dashed-dotted curve to $t_0 = 10$ and the solid curve to $t_0 = 50$. Domain below the curves is stable ($\lambda < 0$), while the instability pertains to the *stretching* mode.

$k = 0$ gives

$$Ma_n \sim \frac{2(2+\chi Sh)W}{\left(2\theta_0(2+\chi Sh) - 2\theta_0' - \theta_0''\right)|_{z=0}} \tag{20}$$

The Ma_n corresponding to marginal stability limit at $k \to 0$ is an increasing function of t_0. This long-wave *deformational* instability is driven by local solutal concentration gradients diminishing with t_0 and, as it follows from Eq. (20), the critical value of Marangoni number at

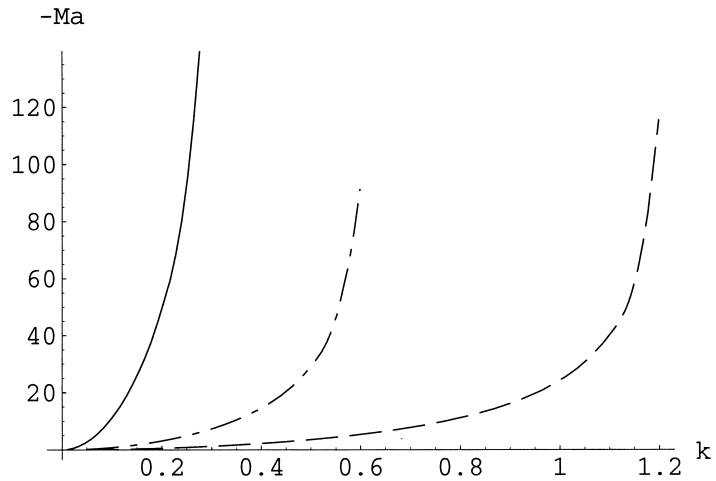

Fig. 2. Neutral stability curves for case (ii) — solute adsorbs by the liquid phase, $W = 500$, $Sc = 100$ and $m * Sh = 5$. The dashed curve relates to the reference time $t_0 = 2.5$, the dashed-dotted curve to $t_0 = 10$ and the solid curve to $t_0 = 50$. Domain right to the curves is stable ($\lambda < 0$), while the instability pertains to the *squeezing* mode.

$k \to 0$ diverges as $t_0 \to \infty$. For increasing times t_0, critical wave number $k_{cr}(t_0)$ slightly decreases while the corresponding $Ma_{cr}(t_0)$ has a minimum which relates to the dash-dotted curve in Fig. 1. The finite wavelength instability gives rise to cellular convection. Initially, when the changes in θ_0 occur only near the interfaces, small-scale convection cells will originate high velocity gradients which result in higher viscous dissipation. So the instability will be retarded by viscosity. As θ_0 develops and becomes less steep, the transverse scale of the convection cells grow and the viscous dissipation diminishes, so the corresponding Ma_{cr} decreases. At some time $t_{0_{cr}}$, the convective layers, which have been originally formed near the two interfaces without interaction with each other, merge and the convection sets in the whole liquid sheet. When $t_0 > t_{0_{cr}}$ the Marangoni effect driving the convection diminishes and $Ma_{cr}(t_0)$ increases (Fig. 1, solid line). For the initial times $t_0 < t_{0_{cr}}$ an observed scenario for the finite length-scale convection is in agreement with previous results of Dijkstra and van de Vooren (1985) who considered the instability of an undeformed liquid–gas interface between semi-infinite phases due to the Marangoni convection. In the latter formulation the corresponding Ma_{cr} is monotonic decreasing function of t_0, while the wavelength of the most dangerous perturbation grows. In case (ii) the system looses its stability through a so called *squeezing*, (SQ) or *varicose* mode ($H_+ = -H_-$). The system is unconditionally unstable to the long wavelength perturbations corresponding to $k = 0$ for any Ma number (Fig. 2). The latter result is qualitatively the same as in a similar problem considered by Oron et al. (1995) where a free deformable liquid sheet exposed to an external temperature gradient is found to be unconditionally unstable to the long wavelength perturbations. Note, also, that the region of unstable Ma numbers shrinks as t_0 increases. The reason for this is the diminishing of the Marangoni effect driving the instability. When there is no solutal transfer, the liquid sheet exhibits no instability for all $W > 0$. It is well known that the long wavelength SQ mode of instability most directly leads to the film rupture. Let us discuss the relative difference in stability of the two cases to the SQ mode of perturbations on the physical grounds. First, consider case (i). The SQ perturbation of the interfaces will result in higher concentration of solute in thicker regions of the sheet and in lower concentration of it in thinner regions of the sheet due to the solutal transfer across the interfaces toward the gas phases. An induced solute concentration gradient along the interfaces will set them into motion, and, consequently, liquid will be dragged into the thinner regions of the liquid sheet and out the thicker regions of the latter. This flow will retard the deformation the initial deformation. In case (ii) the SQ mode will give rise to opposite effect: the transfer of solute into the liquid phase will result in its higher concentration in the thin regions of the liquid sheet and its lower concentration in thicker regions of the liquid sheet. An induced Marangoni flow will enhance the stationary development of the initial deformation since the liquid will be dragged into the thicker region and out the thinner region of the liquid sheet. Actually, in case (i) the long wavelength SQ mode does not lead to instability, while in case (ii) the instability onset occurs at $k \to 0$ at any t_0 for every finite Ma number (see Fig. 2). *Thus, the model presented here suggests that the Marangoni effect can be responsible for the relative difference in stability of the liquid sheet, sandwiched between two gas phases, due to the direction of transfer*. These results of the linear stability analysis are in qualitative agreement with experiments on bubble or drop coalescence. Also, the monotonic increase in long wavelength limit of instability with t_0, for case (i) (solute

is transferred towards the gas phase, see Fig. 1) is in agreement with the stabilizing effect of bubbles' age on coalescence observed by Ueyama et al. (1993).

An oscillatory instability was not found, probably, due to the symmetry of the reference quiescent state. We believe that there is an overstability in a case of the non-symmetric reference solute profile. An existence of an overstability was shown by Oron et al. (1995) for the case of an applied external temperature gradient and by Braverman and Nepomniashchy (1997) for the case of free deformable liquid sheet with uniform exothermic reaction taking place in it.

Acknowledgements

The author would like to thank Dr. A.A. Golovin and Prof. A. Nir for helpful discussions during the course of this investigation.

References

Braverman, L., Nepomniashchy, A.A., 1997. Private Communication.

Carslaw, H.S., Jaeger, J.C., 1960. Conduction of Heat in Solids. Clarendon Press, Oxford.

Danov, K.D., Gurkov, T.D., Dimitrova, T., Ivanov, I.B., Smith, D., 1997. Hydrodynamic theory for spontaneously growing dimple in emulsion films with surfactant mass transfer. J. Colloid Interface Sci. 188, 313–324.

Dijkstra, H.A., van de Vooren, A.I., 1985. Initial flow development due to Marangoni convection in a mass transfer system. Int. J. Mass Transfer 28, 2315–2322.

England, D.C., Berg, J.C., 1971. Transfer of surface-active agents across a liquid–liquid interface. AIChE J. 17, 313–322.

Gourdon, G., Casamatta, G., 1991. Influence of mass transfer direction on the operation of a pulsed sieve-plate pilot column. Chem. Eng. Sci. 46, 2799–2808.

Groothuiz, H., Zuiderweg, F.G., 1960. Influence of mass transfer on coalescence of drops. Chem. Eng. 12, 288–289.

Hennenberg, M., Sorensen, T.S., Sanfeld, A., 1977. Deformational instability of a plane interface with transfer of matter — Part 1. Non-oscillatory critical states with linear concentration profile. J. Chem. Soc. Farad. Trans. II 73, 48–66.

Jeffreys, G.V., Lawson, G.B., 1965. Effect of mass transfer on the rate of coalescence of single drops at a plate interface. Trans. Inst. Chem. Engrs. 43, 294–298.

Lavrenteva, O.M., Leshansky, A.M., Nir, A., 1999. Spontaneous thermocapillary interaction of drops, bubbles and particles: unsteady convective effects at low Peclet number. Phys. Fluids A 11, 1768–1780.

Sorensen, T.S., Hennenberg, M., Sanfeld, A., 1977. Deformational instability of a plane interface with perpendicular linear and exponential concentration gradients. J. Colloid Interface Sci. 61, 62–76.

Oron, A., Deissler, R.J., Duh, J.C., 1995. Marangoni convection in a liquid sheet. Adv. Space. Res. 16, 83–86.

Rabinovich, Struchenko, 1993. Inter-phase instability in absorbing gas in liquid layer. J. Phys. Chem. 67, 567–570 (in Russian).

Slavtchev, S., Honnenberg, M., Legros, G.-C., Lebon, G., 1998. Stationary solutal Marangoni instability in two-layer system. J. Colloid Interface Sci. 203, 354–368.

Sternling, C.V., Scriven, L.E., 1959. Interfacial turbulence: hydrodynamic instability and the Marangoni effect. AIChE J. 5, 514–523.

Ueyama, K., Saeki, M., Matsukata, M., 1993. Development of system for measuring bubble coalescence time by using a laser. J. Chem. Eng. of Japan 26, 308–314.

Velev, O.D., Gurkov, T.D., Borwankar, R.P., 1993. Spontaneous cyclic dimpling in emulsion films due to surfactant mass transfer between the phases. J. Colloid Interface Sci. 159, 497–501.